FORMATION OF CO_2 HYDRATE IN PURE AND SEA WATERS

KAZUNARI OHGAKI*, YOSHIHIRO MAKIHARA AND KIYOTERU TAKANO

Department of Chemical Engineering, Osaka University, Toyonaka, Osaka 560

Key Words: Phase Equilibrium, High Pressure, Thermodynamics, Phase Behavior, Gas Hydrate

The formation of CO_2 hydrates in both pure and sea waters along the three-phase coexistence of CO_2, H_2O, and hydrate is measured by use of a convenient temperature-cycle method proposed in the present study. Four kinds of three-phase coexisting curves are investigated in the temperature range from 270 to 283 K and pressures up to 9 MPa. By applying the Langmuir adsorption model based on statistical thermodynamics, the three-phase coexisting pressures obtained are correlated satisfactorily. The enthalpy changes of hydration in both systems are calculated from the Clapeyron equation of the three-phase coexisting curve. The apparent rate constant of hydration is estimated under the assumption of pseudo-first order reaction with respect to CO_2 concentration.

Introduction

The global greenhouse effect of CO_2 has attracted the attention of many people as a worldwide problem. Ideas for CO_2 disposal in the ocean[14] and CO_2 storage on the ocean floor[9, 10] have been proposed recently as one of the projects of holding the CO_2 concentration below a given level. In both proposals, CO_2 hydrates would play an important role in preventing man-made CO_2 from entering the atmosphere.

Hydrates of crystalline substances are composed of an open water network of host water molecules arranged to prepare small and large cages capable of entrapping guest molecules. Larson[6] found the formula to be $CO_2 \cdot 6H_2O$, indicating that there is at least partial occupancy of the smaller cages. However, the kinetics of hydrate formation is not well known at present.

The pressure-temperature data for the three-phase coexistence of CO_2, H_2O, and hydrate were published by von Stackelberg and Muller[18], Unruh and Katz[16], Takenouchi and Kennedy[15], Robinson and Mehta[13], Berecz and Balla-Achs[2], and Ng and Robinson[8]. Their data correspond to the dissociation points of CO_2 hydrates. From the standpoint of phase equilibrium investigation, the formation and dissociation points should agree precisely at a given temperature. However, measurements of formation points are very scarce because the solid formation behaviour is a rather complicated phenomenon both experimentally and theoretically.

In the present study, both formation and dissociation points have been measured in addition to the stationary point of the reaction, because the hydration rate at the formation point is essential to our object of CO_2 storage on the ocean floor.

* Received April 5, 1993. Correspondence concerning this article should be addressed to K. Ohgaki.

1. Experimental

1.1 Apparatus

A schematic diagram of the apparatus used in this study is shown in **Fig. 1**. The apparatus consists of four major sections: a high-pressure view cell equipped with a magnetic stirrer, a pressurizing and supplying system, a temperature programing and control system, and a pressure and temperature recording system.

High-pressure view cell The reaction cell **[C]** (ca. 150 cm^3 and max. 15 MPa) is made of stainless steel and has a pair of windows on opposite sides which permits observation of phase behaviour. The inner volume of the cell is calibrated by weighing on a precision balance (max. 3 kg, Cho Balance). The contents of the cell are agitated by a magnetic stirrer (Corning PC-520) **[N]** to help establish equilibrium; a cross-type rotator coated with Teflon works at a desired speed (max. 800 rpm).

Supply system The CO_2 charging system consists of a small gas cylinder (Whitey 304L-HDF4) **[H]** for weighing the total amount of CO_2 supplied to the cell, a high-pressure pump (Shimadzu LC6A) **[L]**, and a compensator **[G]** for weighing the small amount of CO_2 retained in the stainless steel line between valve **[1]** and valve **[4]**. The water-charging system is essentially the same as the above. Before the desired amount of CO_2 is charged, a known amount of H_2O is supplied in excess of the stoichiometric proportion under vacuum. All valves used in this experiment are diaphragm valves (Nupro SS-DLS4) to avoid oil contamination.

Temperature programing system An aqueous diethylene glycol bath **[B]** is kept previously at a somewhat elevated temperature (2-3 K higher than expected temperature) for a period of 2-3 hours for complete saturation. With a gradient of 0.3 K per hour, the temperature is lowered continuously until a rapid pressure reduction is recorded. The temperature is then kept constant at that point over a period of more than 15 hours to obtain iso-

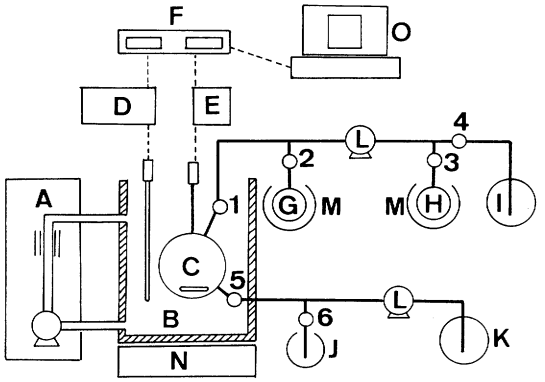

Fig. 1 Schematic diagram of experimental apparatus for observing phase behaviour of gas hydrate
A: programing thermocontroller;
B: aqueous dimethylene glycol bath;
C: high-pressure view cell; D: thermometer;
E: pressure gage; F: recorder;
G: compensator for gas line; H: weighed gas cylinder;
I: gas cylinder; J: compensator for liquid line;
K: water reservoir; L: high-pressure pump;
M: liquid nitrogen bath; N: magnetic stirrer;
O: computer; 1-5: diaphragm valves

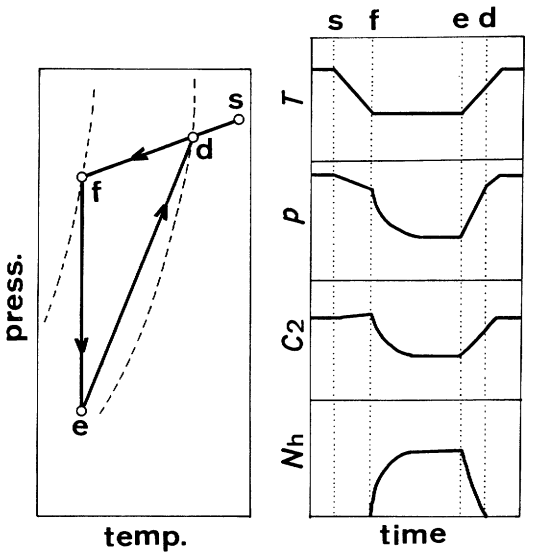

Fig. 2 Working diagram of *T*-cycle method for measuring formation and dissociation of hydrates

thermal reaction rates. Finally, the temperature is increased to the starting point with the same gradient. A programing thermo-controller (Taitec PU-9) **[A]** has an accuracy of 0.05 K. As the cycle is repeated several times for each mixture, we call the procedure the "*T*-cycle" method hereafter.

Recording system The system pressure was measured using a calibrated pressure transducer (Valcom VPRT) **[E]** located very close to the cell. The accuracy of pressure measurement was estimated to be within 5 kPa. The temperature was measured with an accuracy of ±0.01 K by using a thermometer (Takara D-641) **[D]**. Data of both quantities were stored continuously in a recorder (Yokogawa LR4120) **[F]** and a personal computer **[O]**.

1.2 *T*-cycle method

A working diagram of the *T*-cycle method for determining the formation, dissociation, and stationary point of CO_2 hydration is schematically shown in **Fig. 2**.

A CO_2-H_2O (or sea water) mixture, where the quantity of each component is known previously, is in vapor-liquid equilibrium at a starting point (s) under isothermal condition. The system temperature is reduced gradually with a temperature gradient of 0.3 K/h until a rapid pressure depression is observed. This point (f) is regarded as a formation point of hydrates with two coexisting fluid phases. To obtain a good reproducible datum on hydrate formation, we have paid attention to the following items. The temperature gradient of cooling should be smaller than 0.6 K/h, and the rotational speed of the magnetic rotator must be higher than 400 rpm in our experiment. Especially, the agitation should be performed so strongly as to prevent the crystallization of hydrates at only the interface between the two fluid phases.

The temperature is kept constant at the point of rapid pressure depression over a period of 15 hours. Although hydration is nearly finished in the first 2-3 hours, the mixture is left to stand undisturbed overnight. In general, the reaction starts rapidly and the rate then decreases with time until maximum sorption is attained. This point (e) is adopted as the stationary point of the reaction. It is very important that the quantity of H_2O is far in excess of the stoichiometric proportion of $CO_2 \cdot 6H_2O$, because a sudden increase in pressure would result from a very large heat of formation in a higher pressure range than the quadruple point.

Temperature is increased again with the same gradient of 0.3 K/h. On the way to point (s) from (e), there is a turning point (d) on the pressure-time diagram, although the change of pressure gradient at point (d) is not so clear in comparison with that of point (f). The last particle of hydrates disappears on heating at point (d), and we adopt this point as a dissociation point of hydrates. As one cycle of the "*T*-cycle" method is usually complete in a period of about 35 hours, one mixture requires a week for several cycles.

The "*T*-cycle" method in the present study is an effective and convenient technique for determining the formation and dissociation points of hydrates because the ordinary isobaric method requires very accurate pressure control, which makes the procedure troublesome. As the volume of the high-pressure cell and the quantities of CO_2 and H_2O charged in the cell are known, the concentration of CO_2 in the solution, C_2, and the amount of forming CO_2 hydrate, N_h, are calculated from the material balance assuming that the mole fraction of H_2O in the gas phase is zero. These variables, including temperature and pressure, are plotted schematically as a function of elapsed time on the right-hand side of Fig. 2.

1.3 First-freezing point method

The three-phase coexisting lines of (hydrate, CO_2-

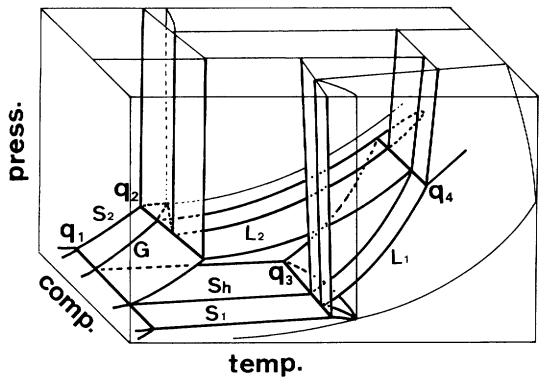

Fig. 3 Schematic diagram of pressure-temperature-composition of CO_2 hydrate system
Symbols of single phase: S_h = hydrate; S_1 = ice; S_2 = solid CO_2; L_1 = H_2O-rich liquid; L_2 = CO_2-rich liquid; G = gas
quadruple points: $q_1 = S_hS_1S_2G$; $q_2 = S_hS_2L_2G$; $q_3 = S_hS_1L_1G$; $q_4 = S_hL_1L_2G$

rich liquid, and CO_2-rich gas) and (H_2O-rich liquid, CO_2-rich liquid, and CO_2-rich gas) are measured by the first-freezing point method[3], because the phase transition in this region does not show a large pressure reduction. As the first-freezing point method was described in a previous paper[19], the details are not mentioned here. First, starting from the gas-liquid equilibrium, which is slightly above the expected three-phase coexisting line (both in pressure and temperature), the system temperature is lowered slowly at a rate of 0.3 K/h. When a new phase (solid or liquid) appears, the three-phase coexisting point is obtained.

1.4 Materials

Research grade CO_2 (purity 99.99+ mol %) was obtained from Takachiho Trading Co., Ltd. and used without further purification. Water was purified by distillation followed by deionization. Artificial sea water, having a concentration of 1.9 mass% of Cl (NaCl: 2.35, $MgCl_2$: 0.498, Na_2SO_4: 0.392, $CaCl_2$: 0.110 mass%, etc.), was supplied from Senju Pharma. Co. Ltd.

2. Experimental Results

2.1 Pressure-temperature relation

The pressure-temperature-composition information for the H_2O-CO_2-hydrate system is schematically described with a 3-dimensional space as shown in **Fig. 3**. The diagram, essentially the same as those for the pure water and sea water systems, has at least four quadruple points and twelve three-phase coexisting curves. In the present study, the four three-phase coexisting curves originating from the quadruple point of q_4, S_h-L_1-G, S_h-L_1-L_2, S_h-L_2-G, and L_1-L_2-G (refer to the caption of Fig. 3), are measured for the pure water and sea water systems.

Table 1 summarizes the experimental data for CO_2 hydration in the pure water system. The dissociation data obtained from the *T*-cycle method agree within experimental error with those of Unruh and Katz[16], Robinson and Mehta[13], Berecz and Balla-Achs[2], and Ng and Robinson[8]. The formation data shift toward the lower temperatures. The temperature difference between formation and dissociation is about 2 K at the same pressure. The formation curve obtained in the present study has good

Table 1. Pressure and temperature relation of three-phase coexistence for the pure water system

T [K]	*p* [MPa]	*T* [K]	*p* [MPa]	*T* [K]	*p* [MPa]
T-cycle method (formation)					
S_h-L_1-G curve					
273.36	1.338	274.03	1.509	274.94	1.651
276.01	1.839	276.29	1.971	276.56	1.966
276.57	2.005	276.98	2.108	277.51	2.238
278.13	2.482	278.69	2.656	278.76	2.604
279.23	3.030	279.50	3.019	280.13	3.228
280.34	3.395	280.79	3.667	281.10	4.085
S_h-L_1-L_2 curve					
281.52	4.386	281.14	5.596	281.28	5.693
281.70	6.861	282.21	8.615		
T-cycle method (dissociation)					
S_h-L_1-G curve					
273.95	1.347	275.37	1.544	276.82	1.977
277.82	2.116	279.42	2.674	281.21	3.279
281.79	3.831				
S_h-L_1-L_2 curve					
283.23	4.541	283.25	6.306	283.59	8.930
T-cycle method (stationary point)					
S_h-L_1-G curve					
275.97	1.740	276.54	1.881	277.45	2.126
278.66	2.497	278.75	2.499	279.16	2.614
280.33	3.076				
first freezing-point method					
S_h-L_2-G curve					
274.92	3.637	275.90	3.730	276.85	3.823
277.84	3.910	278.80	4.012	279.82	4.115
280.82	4.222	281.27	4.281		
L_1-L_2-G curve (absence of hydrate)					
283.07	4.485	283.15	4.495	283.46	4.524
283.95	4.578	284.47	4.636	285.43	4.748
286.38	4.860	287.39	4.977	288.40	5.089
289.37	5.216				

The S_h-L_2-G data with the first freezing point-method correspond to the formation curve. The formation and dissociation points with the *T*-cycle method do not always make a pair in the present table.

Table 2. Pressure and temperature relation of three-phase coexistence for the sea water system

T [K]	p [MPa]	T [K]	p [MPa]	T [K]	p [MPa]
T-cycle method (formation)					
S_h-L_1-G curve					
273.87	1.710	273.95	1.711	275.57	2.095
275.66	2.103	277.43	2.652	277.48	2.654
278.79	3.165	279.67	3.537	279.74	3.549
280.08	3.970	280.36	3.980		
S_h-L_1-L_2 curve					
280.57	4.891				
T-cycle method (dissociation)					
S_h-L_1-G curve					
274.75	1.730	276.57	2.121	278.34	2.677
279.68	3.182	280.42	3.561	281.28	4.014
281.46	4.020				
S_h-L_1-L_2 curve					
282.01	5.436				
T-cycle method (stationary point)					
S_h-L_1-G curve					
273.78	1.590	275.56	1.945	277.47	2.532
278.70	2.986	279.73	3.426	280.03	3.625
280.36	3.743				
first freezing-point method					
S_h-L_2-G curve					
279.62	4.1494				
L_1-L_2-G curve (absence of hydrate)					
281.59	4.361	282.56	4.464	283.52	4.573
284.15	4.681				

The data on S_h-L_2-G and L_1-L_2-G curves are almost the same as those for the pure water system.

reproducibility under conditions of small temperature gradient and enough agitation. The three-phase coexisting curves obtained with the first-freezing point method correspond, in principle, to the formation data.

Table 2 summarizes the data of the sea water system. The three-phase coexisting curves (S_h-L_1-G and S_h-L_1-L_2) of the sea water system is 1.5-2 K lower than that of the pure water system. This phenomenon is similar to the solubility depression based on the salting-out behavior. The three-phase coexisting curves of S_h-L_2-G and L_1-L_2-G of the sea water system are equivalent to those of the pure water system.

3. Thermodynamics of CO_2 Hydration

3.1 Adsorption model for CO_2 hydrate

By applying the Langmuir adsorption model, van der Waals and Platteeuw[17] proposed a method for calculating fundamental thermodynamic properties of hydrates. Marshall, Saito and Kobayashi[7] and Parrish and Prausnitz[11] pointed out that the Kihara potential model is quite effective for describing the pressure-temperature diagram of non-sphere gas hydrates. Recently John and Holder[4] and John, Paradopoulos and Holder[5] have developed a model which incorporates the effect of spherical asymmetry of guest molecules. Their model is effective for CO_2 hydrate because the rotational motion of linear CO_2 molecules in hydrate cages is restricted by H_2O molecules as reported by Ratcliffe[12].

Introducing a hypothetical empty hydrate state, the fundamental relation of chemical potential is written as

$$\Delta\mu = \mu^{\mathrm{emp}}(T, p) - \mu^{\mathrm{hyd}}(T, p, x) = -RT\Sigma\nu_i \ln(1 - \Sigma\theta_{ij}) \quad (1)$$

where $\Delta\mu$ is the chemical potential difference between the occupied hydrate and the hypothetical empty hydrate lattice, x is the mole fraction of gas component in the liquid phase, R is the gas constant, ν_i is the crystallographic constant of the cages, and θ_{ij} is the cage occupation probability of guest molecules. The analogous description of occupation probability is applied to the Langmuir adsorption,

$$\theta_{ij} = \alpha c_{ij} f_j / (1 + \Sigma\alpha c_{ij} f_j) \quad (2)$$

where c_{ij} is the Langmuir constant, f_j is the fugacity calculated from the equation of state[1], and α, being independent of temperature, is the shape factor of a linear molecule. The Langmuir constant is written (without subscripting) as

$$c = 1/RT \int \exp(-u/RT)\,\mathrm{d}v \quad (3)$$

where u is the total smoothed-cell potential proposed by John and Holder[4]. The Kihara potential parameters obtained from the second virial coefficient data were used for calculation of CO_2-H_2O interaction in the hydrate cages. To correct the restricted motion of CO_2 molecules in the cages, an additive parameter, α, is introduced. The parameter α was adjusted so that good agreement was obtained between experimental and calculated three-phase co-existing pressures. Other constants reported by John and Holder[4] were applied just as they are. The optimum values of parameters are α = 0.0361, 0.0392, and 0.0378 for formation, dissociation, and stationary point curves, respectively.

The activity of H_2O in the artificial sea water, a_1 (sea), is written by a depression of temperature on the three-phase co-existence at a given pressure.

$$\ln[a_1(\mathrm{sea})/a_1(\mathrm{pure})] = \Delta H(\mathrm{react.})/6R \cdot [1/T(\mathrm{sea}) - 1/T(\mathrm{pure})] \quad (4)$$

Table 3. Correlation constants of apparent Henry constants

system	A [-]	B [-]	p° [MPa]
pure water	–468.4	1.985	2.238
sea water	–616.8	2.624	2.652

Table 4. Constants of the Clapeyron equation for S_h-L_l-G three-phase coexistence
$\ln(p/\mathrm{MPa}) = A + B\ K/T + C \ln(T/\mathrm{K})$

system	curve	A [-]	B [-]	C [-]
pure water	formation	4.8596	–8885.95	4.9764
	dissociation	4.8735	–8895.83	4.9636
	stationary	4.8770	–8894.38	4.9645
sea water	formation	4.8372	–8891.81	5.0125
	dissociation	4.8530	–8893.60	4.9911
	stationary	4.8460	–8892.38	5.0020

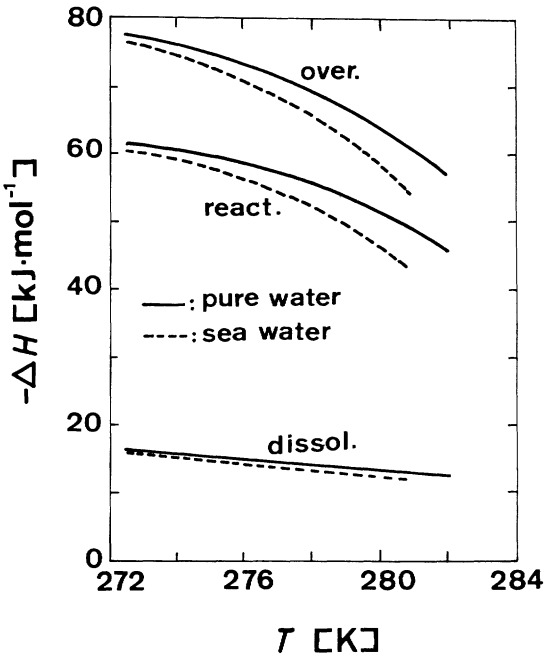

Fig. 4 Enthalpy changes calculated from the Clapeyron equation

As the enthalpy change of $CO_2 \cdot 6H_2O$ formation, ΔH (react.), is evaluated in the present study (see section 3.4), the value of a_1 (sea) is calculated assuming that a_1 (pure) is equal to the mole fraction of H_2O in the pure water system. Finally, the electrolytic effect of artificial sea water on the chemical potential of H_2O is obtained as a polynomial expression.

$$-\Delta\mu_{elec}/RT = -4.805 + 0.003562\,T/\mathrm{K} - 6.573\times10^{-5}\,T^2/\mathrm{K}^2 \quad (5)$$

After the correction of the electrolytic effect on the chemical potential depression of H_2O, each optimum value for the pure water system is effective for the sea water system. The averaged standard deviations of pressure correlations are ±4.3 kPa for the pure water and sea water systems. The composition of CO_2 hydrate calculated from the cage occupation probability in the adsorption model is in good agreement with the ratio of CO_2 : H_2O = 1 : 6

3.2 Solubility of CO_2

As explained in the experimental section, the volume of the high-pressure cell and the total amount of each component charged are known previously. To estimate the CO_2 concentration in the fluid, we introduce the assumptions that the partial molar volume of CO_2 dissolved in the fluid is equal to the saturated liquid molar volume of pure CO_2 at a given temperature, and that the gas phase in equilibrium is almost pure CO_2. Thus the apparent Henry constants are estimated from the data of gas-liquid equilibrium before hydration occurs. In the present experimental conditions, the apparent Henry constant can be correlated as a function of temperature and pressure.

$$H(T,p)/\mathrm{MPa} = (A + B\,T/\mathrm{K})\exp[-V_2(p-p^0)/RT] \quad (6)$$

where $H(T, p)$ is the apparent Henry constant, which depends on pressure as well as temperature and V_2 is the saturated liquid molar volume of CO_2 at a given temperature. **Table 3** summarizes the values of constants which are applicable in this experimental range for the pure water and sea water systems. As the quantities of CO_2 in both the gas and liquid phases are calculated from these assumptions, the mole fraction of CO_2 dissolved in the fluid phase, x_2, is also obtainable.

$$x_2 = f(T,p)/H(T,p) \quad (7)$$

where $f(T, p)$ is the fugacity of CO_2, which is calculated from the recommended equation of IUPAC[1].

3.3 Kinetics of hydration

According to Larson[6], the hydration of CO_2 is simplified,

$$CO_2\,(\text{gas or liquid}) + 6H_2O\,(\text{liquid}) = CO_2 \cdot 6H_2O \quad (8)$$

where the state of CO_2 fluid depends on the pressure at a given temperature. The change in enthalpy when one mole of CO_2 is taken from the gas phase and adsorbed within a cage of hydrate is calculated from the Clapeyron equation.

$$dp/dT = \Delta H/(T\Delta V) \quad (9)$$

As the empirical correlation for three-phase coexistence is given by Eq. (10) and ΔV is calculated from the equation of state[1], the value of ΔH is obtained from the plot of the logarithm of p and $1/T$.

$$\ln(p/\mathrm{MPa}) = A + B\,\mathrm{K}/T + C\ln(T/\mathrm{K}) \quad (10)$$

Table 4 summarizes the values of constants in Eq. (10) for formation, dissociation, and stationary points of pure water and sea water systems. In the higher-pressure

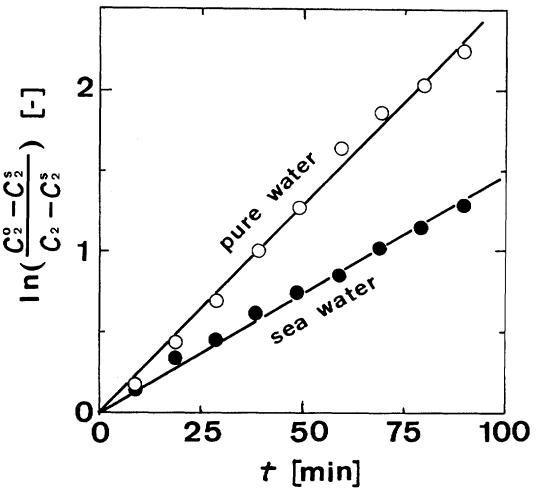

Fig. 5 Plots of ln $\{(C_2^0 - C_2^s)/(C_2 - C_2^s)\}$ against t
pure water: $T = 277.51$ K and $p = 2.238$ MPa
sea water: $T = 277.43$ K and $p = 2.652$ MPa

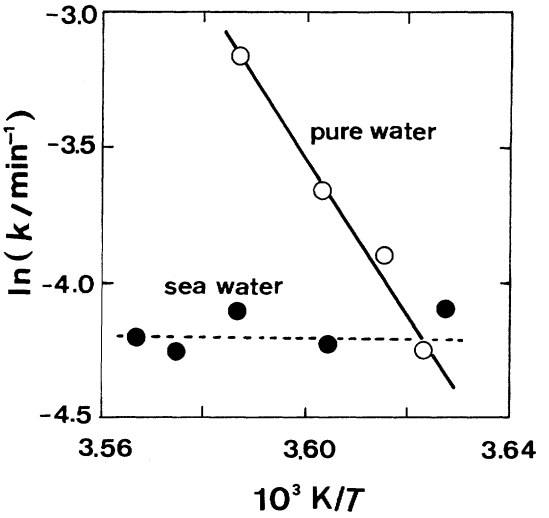

Fig. 6 Arrhenius plots of apparent rate constant of hydration
pure water: $k = 5.92 \times 10^{43} \exp(-241\ \text{kJ·mol}^{-1}/RT)\ \text{min}^{-1}$
sea water: $k = 0.014 \pm 0.003\ \text{min}^{-1}$

region than the quadruple point (S_h-L_1-L_2-G), the coexisting pressure on the S_h-L_1-L_2 curve is almost perpendicular. No empirical correlation was applied to the S_h-L_1-L_2 curve because the higher-pressure data in this study are not adequate.

Figure 4 shows the enthalpy changes of reaction between water and gaseous CO_2 in the formation process. The solid lines denote the pure water system and the dashed lines are the sea water system. The values of dp/dT were calculated from Eq. (10) of the stationary point curve. The enthalpy change of dissolution, ΔH (dissol.), was calculated from the temperature dependence of solubilities. The enthalpy change of reaction, ΔH (react.), was defined as the difference between ΔH (over.) and ΔH (dissol.). It is remarkable that the value of ΔH (react.) at 273.15 K is still 60 % larger than the enthalpy change of the melting of $6H_2O$.

3.4 Evaluation of hydration rate

As the concentrations of CO_2 and CO_2 hydrate at a given temperature are calculated from a datum set of the T-cycle method, the hydration rate is obtained in the process from the formation point to the stationary point under the assumption of pressure independence. The apparent rate constant of the first-order reaction was calculated from the slope of the straight line shown in **Fig. 5**.

$$d C_h / dt = k (C_2 - C_2^s) \tag{11}$$

where k is the apparent rate constant and C_2^s is the saturated concentration of CO_2 at the stationary point. The rate constant of the pure water system is larger than that of the sea water system in the higher-temperature range while both constants agree approximately in the lower-temperature range. The apparent rate constants of the pure water system is given by Eq. (12).

$$k = k^0 \exp(-E_a / RT) \tag{12}$$

where the values of k^0 and E_a are 5.92×10^{43} min^{-1} and 241 kJ/mol, repectively. On the other hand, the value of k in the sea water system, being independent of temperature in the present experimental region, is 0.014 ±0.003 min^{-1} as shown in **Fig. 6**. This finding can be explained in terms of the existence of ionic substances in sea water. However, further investigation on the hydration mechanism in electrolytic solutions is necessary for detecting the accurate hydration rate.

Conclusion

The formation, dissociation, and stationary points along the three-phase coexistence curves in the pure water and sea water systems were measured by the T-cycle method presented in the present study. Each curve involving a water-rich liquid phase in the sea water system shifts about 2 K toward the lower side than that in the pure water system at the same pressure.

The hydration in both systems can be assumed to be a pseudo-first order reaction with respect to CO_2 concentrations. However, further study of some ionic substances is necessary for investigating the mechanism of the hydration of sea water.

Acknowledgment

The authors wish to thank Dr. Masato Moritoki of Kobe Steel Ltd. for his useful discussions about high-pressure equipment. They are also grateful to the Institute for Laser Technology and the Kansai Electric Power Company, Inc. for their financial support. This research was supported by a Grant-in-Aid for the Scientific Research Fund in 1992 (Project No. 04238213) from the Ministry of Education, Science and Culture, Japan.

Nomenclature

a	=	activity	[-]
C	=	concentration of CO_2	[kmol/m^3]
c	=	Langmuir constant	[MPa^{-1}]
E_a	=	activation energy	[kJ/mol]
f	=	fugacity	[MPa]

ΔH	=	enthalpy change	[J/mol]
H	=	apparent Henry constant	[MPa]
k	=	apparent rate constant of hydration	[min^{-1}]
N	=	amount of hydrate	[mol]
p	=	pressure	[MPa]
R	=	gas constant	[J/mol·K]
T	=	temperature	[K]
t	=	time	[min]
u	=	cell potential	[J/mol]
V	=	molar volume	[m^3/mol]
v	=	molar volume of hydrate cage	[m^3/mol]
x	=	mole fraction	[-]
α	=	shape factor (fitting parameter)	[-]
θ	=	cage occupation probability	[-]
μ	=	chemical potential of hydrate	[J/mol]
ν	=	number of cages per H_2O molecule	[-]

G	=	symbol of gas phase
L	=	symbol of liquid phase
S	=	symbol of solid phase

<Subscripts>

1	=	H_2O
2	=	CO_2
h	=	hydrate
i, j	=	cage type
diss	=	dissociation
form	=	formation
elec	=	electrolytic term

<Superscripts>

emp	=	empty hydrate cage
hyd	=	filled hydrate cage
s	=	stationary point
0	=	initial state

Literature cited

1) Angus, S., B. Armstrong and de K.M. Reuck: "International Thermodynamic Tables of The Fluid State, Carbon Dioxide", Pergamon, Oxford (1976)
2) Berecz, E. and M. Balla-Achs: "Gas Hydrates", Studies in Inorganic Chemistry 4, Elsevier, Amsterdam (1983)
3) Cheong, P.L., D. Zhang, K. Ohgaki and B.C.-Y. Lu: *Fluid Phase Equilib.*, **29,** 555-562 (1986)
4) John, V.T. and G.D. Holder: *J. Phys. Chem.*, **89,** 3279-3285 (1985)
5) John, V.T., K.D. Papadopoulos and G.D. Holder: *AIChE J.*, **31,** 252-259 (1985)
6) Larson, S.D.: Ann Arbor, Mich., Doctoral Dissertation (1955)
7) Marshall, D.R., S. Saito and R. Kobayashi: *AIChE J.*, **10,** 202-205 (1964)
8) Ng, H.-J. and D.B. Robinson: *Fluid Phase Equilib.*, **21,** 145-155 (1985)
9) Ohgaki, K. and Y. Inoue: *Kagaku Kogaku Ronbunshu,* **17,** 1053-1055 (1991)
10) Ohgaki, K. and T. Akano: *Energy & Resources,* **13,** 375-383 (1992)
11) Parrish, W.R. and J.M. Prausnitz: *Ind. Eng. Chem. Proc. Des. Dev.,* **11,** 26-35 (1972)
12) Ratcliffe, C.I. and J.A. Ripmeester: *J. Phys. Chem.*, **90,** 1259-1263 (1986)
13) Robinson, D.B. and B.R. Mehta: *J. Can. Pet. Technol.*, **10,** 33-35 (1971)
14) Steinberg, M., H.C. Cheng and F. Horn: A System Study for the Removal, Recovery and Disposal of Carbon Dioxide from Fossil Fuel Power Plants in the U.S., Brookhaven National Laboratory (1984)
15) Takenouchi, S. and G.C. Kennedy: Geology. Notes no. 293, Inst. of Geophys., Univ. of California, 383-390 (1964)
16) Unruh, C.H. and D.L. Katz: *J. Petrol. Tech.*, **1,** 83-86 (1949)
17) van der Waals, J.H. and J.C. Platteeuw: *Adv. Chem. Phys.*, **2,** 1-57 (1959)
18) von Stackelberg, M.W. and H.R. Muller: *J. Chem. Phys.*, **19,** 1319-1320 (1951)
19) Yamamoto, S., K. Ohgaki and T. Katayama: *J. Supercrit. fluids,* **2,** 63-72 (1989)